NOTES AND CORRESPONDENCE

Polynomial Approximation of the Optical Properties of Water Clouds in the 8–12-μm Spectral Region

PETR CHÝLEK* AND PETER DAMIANO

Atmospheric Science Program, Department of Physics and Oceanography, Dalhousie University, Halifax, Nova Scotia, Canada

DAT NGO

Department of Physics, New Mexico State University, Las Cruces, New Mexico

R. G. PINNICK

Atmospheric Science Laboratory, White Sands Missile Range, New Mexico

15 August 1991 and 23 December 1991

ABSTRACT

We have developed a simple approximation for the absorption, extinction and scattering coefficients, infrared emittance, single-scattering albedo, and asymmetry factor of water clouds within the 8–12-μm spectral region. The aforementioned cloud-scattering characteristics are obtained as continuous functions of the wavelength λ, liquid water content W, effective radius r_{eff}, and effective variance v_{eff} of the droplet-size distribution. The accuracy of the proposed approximation is shown to be within 6% for most types of water clouds when compared to the exact Mie theory calculation and integration over the size distribution. At the same time the required computer time is reduced by a factor of 10^2–10^3.

1. Introduction

The purpose of this note is to present a simple analytical approximation for the radiative characteristics (absorption coefficient k_{abs}, emittance ϵ, extinction coefficient k_{ext}, single-scattering albedo ω_0, and the asymmetry parameter g) of water clouds in the 8–12-μm wavelength region. We seek an approximation that is computationally fast (does not require any Mie calculation) and provides the listed radiative characteristics to within 6% accuracy, when compared with the exact Mie calculation integrated over typical size distributions. The approximation should lead to simple analytical expressions for the absorption coefficient, the extinction coefficient, the single-scattering albedo, and the asymmetry factor as a function of the wavelength λ, the liquid water content W, and two additional parameters specifying the cloud-droplet-size distribution.

Water clouds' infrared emittance is usually written in the no-scattering approximation (e.g., Hunt 1973; Paltridge and Platt 1976; Stephens et al. 1990) in the form

$$\epsilon = 1 - e^{-k_{\text{abs}}z} \tag{1}$$

where z is the cloud's geometrical thickness. The absorption coefficient k_{abs} is defined by

$$k_{\text{abs}}(\lambda) = \pi \int r^2 Q_{\text{abs}}(r, \lambda) n(r) dr \tag{2}$$

where Q_{abs} is the Mie absorption efficiency (e.g., van de Hulst 1957) and $n(r)$ is the cloud-droplet-size distribution.

The extinction coefficient k_{ext}, single-scattering albedo ω_0, and the asymmetry factor g are defined as

$$k_{\text{ext}}(\lambda) = \pi \int r^2 Q_{\text{ext}}(r, \lambda) n(r) dr \tag{3}$$

$$\omega_0 = \frac{k_{\text{ext}} - k_{\text{abs}}}{k_{\text{ext}}} \tag{4}$$

$$g(\lambda) k_{\text{sc}}(\lambda) = \pi \int r^2 g_r(r, \lambda) Q_{\text{sc}}(r, \lambda) n(r) dr \tag{5}$$

with the Q_{sc} and Q_{ext} being the Mie scattering and extinction efficiency and g_r the single-particle asymmetry factor (e.g., van de Hulst 1957). The scattering coefficient $k_{\text{sc}} = k_{\text{ext}} - k_{\text{abs}}$.

* Also affiliated with the Atmospheric Sciences Research Center and Department of Atmospheric Science, SUNY, Albany, NY 12222.

Corresponding author address: Prof. Petr Chýlek, Dalhousie University, Atmospheric Science Program, Department of Physics and Oceanography, Halifax, NS, B3H 3J5 Canada.

The often-used parameterization of the cloud infrared emittance as a linear function of liquid water content W is based on the linear approximation of Q_{abs} as a function of the droplet radius r in the form (e.g., Platt 1976; Chýlek 1978; Pinnick et al. 1979; Chýlek and Ramaswamy 1982; Stephens 1984)

$$Q_{abs}(r, \lambda) = a(\lambda)r, \tag{6}$$

where $a(\lambda)$ is a constant (at a considered wavelength λ) determined from the best linear fit to Q_{abs} for values of $r < r_{max}$. The r_{max} is a maximum radius for which (at a given wavelength) the linear fit represents an acceptable approximation. Because the character of the Q_{abs} curve changes with the wavelength, this maximum radius r_{max} depends on the wavelength considered.

Using the parameterization for the absorption efficiency (6) in the integral for the absorption coefficient (2) and the no-scattering emittance approximation (1) leads to the following expressions for the absorption coefficient k_{abs} and the infrared emittance:

$$k_{abs}(\lambda) = 3Wa(\lambda)/4\rho \tag{7}$$

and

$$\epsilon(\lambda) = 1 - \exp[-3Wa(\lambda)z/4\rho], \tag{8}$$

where ρ is the specific density of liquid water.

The linear relationship (6) is reasonably well satisfied for small droplet radii; $r < 9$ μm at the wavelength of $\lambda = 8$ μm and $r < 4$ μm at $\lambda = 12$ μm (Pinnick et al. 1979). However, most clouds have droplet-size distributions considerably exceeding the stated limits on the droplet radius r, and therefore, the use of the aforementioned parameterization is not justified.

To standardize cloud-droplet-size distributions we chose the distributions used in LOWTRAN 7 (Kneyzys et al. 1988; Shettle 1989). These size distributions (Fig. 1) are also very close to those used by Deirmendjian

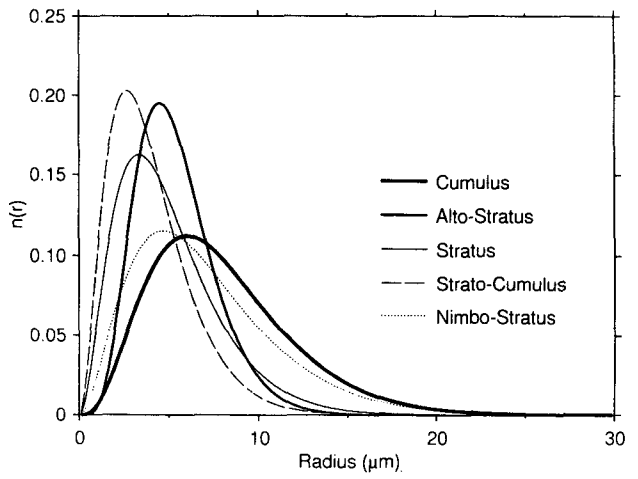

FIG. 1. Cloud-droplet-size distributions used in LOWTRAN models and in this study. The graphs were normalized in such a way that the area under each graph is equal to 1.

TABLE 1. Parameters of droplet-size distributions.

Cloud type	α	β	A	W (g m^3)	r_{eff} (μm)	v_{eff}
Stratus	2	0.6	27.0	0.29	8.33	0.20
Nimbostratus	2	0.425	7.676	0.65	11.76	0.20
Cumulus	3	0.5	2.604	1.00	12.0	0.17
Altostratus	5	1.111	6.268	0.41	7.2	0.125
Stratocumulus	2	0.75	52.734	0.15	6.67	0.20

(1969) and others (e.g., Chýlek and Ramaswamy 1982) in previous studies. We use the gamma-type size distribution (Deirmendjian 1969; Hansen and Travis 1974; Stephen et al. 1990) in the form

$$n(r) = Ar^{\alpha}e^{-\beta r} \tag{9}$$

with the constants A, α, and β listed in Table 1.

The absorption coefficient k_{abs}, calculated exactly by using the Mie theory and numerical integration over the size distribution (2) was compared to the results obtained from (7) for the size distributions given in Table 1. The percentage error of this approximation reaches over 140% (Table 2).

If the Nth-degree polynomial approximation

$$Q_{abs}(r, \lambda) = \sum_{n=0}^{N} a_n(\lambda)r^n \tag{10}$$

is used instead of the linear relationship (6), the region of the validity can be extended to arbitrarily large (depending on N) droplet radii (Chýlek et al. 1992).

The expansion coefficients $a_n(\lambda)$ with $N = 2$ and $N = 10$ were determined by least-squares fit to the Mie absorption efficiency $Q_{abs}(r, \lambda)$ at a given wavelength λ in half-micrometer steps (Tables 2 and 4 of Chýlek et al. 1992). Within the 8–12-μm region the expansion coefficients a_n are slowly varying functions of the wavelength λ. This suggests that within the 8–12-μm region the Q_{abs} may be approximated by a continuous function of two variables, the wavelength λ and radius r in the form

$$Q_{abs}(r, \lambda) = \sum_{n=0}^{N}\sum_{j=0}^{J} a_{nj}r^n\lambda^j. \tag{11}$$

Similar polynomial approximations will be used for the extinction coefficient Q_{ext} and the asymmetry parameter g_r in the form

$$Q_{ext}(r, \lambda) = \sum_{n=0}^{N}\sum_{j=0}^{J} b_{nj}r^n\lambda^j \tag{12}$$

$$(Q_{ext} - Q_{abs})g_r(r, \lambda) = \sum_{n=0}^{N}\sum_{j=0}^{J} c_{nj}r^n\lambda^j \tag{13}$$

where b_{nj} and c_{nj} are the expansion coefficients to be determined from the least-squares fit to the exact Mie calculations of Q_{ext} and $(Q_{ext} - Q_{abs})g_r$.

TABLE 2. Percentage error $(k_{Mie} - k_{abs})/k_{Mie}$ of the $k_{abs} = 3Wa(\lambda)/4\rho$ approximation (7). Values of $a(\lambda)$ used are those given by Pinnick et al. (1979).

λ (μm)	Stratus	Nimbostratus	Cumulus	Altostratus	Stratocumulus
8.0	−6	−22	−22	−0.4	0.4
9.0	−5	−20	−20	0.4	1.2
10.0	−8	−24	−24	−1.9	−0.9
11.0	−25	−53	−54	−14	−12
12.0	−82	−141	−143	−6	−55

2. $N = 4$, $J = 4$ approximation

Numerical calculations indicate that the smallest values of N and J that lead to an accuracy of 6% in k_{abs}, k_{ext}, and g within the 8–12-μm wavelength interval are $N = J = 4$.

Substitution of (11) with $N = J = 4$ and the gamma-type size distribution (9) into (2) for the absorption coefficient k_{abs} leads to

$$k_{abs}(\lambda, r_{eff}, v_{eff}) = \frac{3W}{4\rho}\left[\frac{1}{r_{eff}}\sum_{j=0}^{4} a_{0j}\lambda^j + \sum_{j=0}^{4} a_{1j}\lambda^j + r_{eff}(1+v_{eff})\sum_{j=0}^{4} a_{2j}\lambda^j + r_{eff}^2(1+v_{eff})(1+2v_{eff})\sum_{j=0}^{4} a_{3j}\lambda^j + r_{eff}^3(1+v_{eff})(1+2v_{eff})(1+3v_{eff})\sum_{j=0}^{4} a_{4j}\lambda^j\right]. \quad (14)$$

Similarly, the extinction coefficient and the asymmetry factor g are obtained in the form

$$k_{ext}(\lambda, r_{eff}, v_{eff}) = \frac{3W}{4\rho}\left[\frac{1}{r_{eff}}\sum_{j=0}^{4} b_{0j}\lambda^j + \sum_{j=0}^{4} b_{1j}\lambda^j + r_{eff}(1+v_{eff})\sum_{j=0}^{4} b_{2j}\lambda^j + r_{eff}^2(1+v_{eff})(1+2v_{eff})\sum_{j=0}^{4} b_{3j}\lambda^j + r_{eff}^3(1+v_{eff})(1+2v_{eff})(1+3v_{eff})\sum_{j=0}^{4} b_{4j}\lambda^j\right] \quad (15)$$

$$g(k_{ext} - k_{abs}) = \frac{3W}{4\rho}\left[\frac{1}{r_{eff}}\sum_{j=0}^{4} c_{0j}\lambda^j + \sum_{j=0}^{4} c_{1j}\lambda^j + r_{eff}(1+v_{eff})\sum_{j=0}^{4} c_{2j}\lambda^j + r_{eff}^2(1+v_{eff})(1+2v_{eff})\sum_{j=0}^{4} c_{3j}\lambda^j + r_{eff}^3(1+v_{eff})(1+2v_{eff})(1+3v_{eff})\sum_{j=0}^{4} c_{4j}\lambda^j\right]. \quad (16)$$

The expansion coefficients a_{nj}, b_{nj}, and c_{nj} are listed in Table 3. They were obtained by the least-squares fit to the Mie calculation of the Q_{ext}, Q_{abs}, and $(Q_{ext} - Q_{abs})g_r$ in the radii range $r < 30$ μm. Consequently, the derived expressions (14)–(16) should not be used for the cloud (or fog) size distributions with considerable fraction of droplets having radii $r > 30$ μm.

The effective radius r_{eff} and the effective variance v_{eff} of the size distribution $n(r)$ are defined as (Hansen and Travis 1974)

$$r_{eff} = \frac{\int r^3 n(r)dr}{\int r^2 n(r)dr} \quad (17)$$

$$v_{eff} = \frac{\int (r - r_{eff})^2 r^2 n(r)dr}{\int r_{eff}^2 r^2 n(r)dr}. \quad (18)$$

In the case of the gamma-type size distribution (9) the effective radius and effective variance are given by

$$r_{eff} = \frac{\alpha + 3}{\beta} \quad (19)$$

and

$$v_{eff} = \frac{1}{\alpha + 3}. \quad (20)$$

For the case of lognormal size distribution (e.g., Clark and Whitby 1967; d'Almeida et al. 1991)

$$n(r) = \frac{N_0}{rs\sqrt{2\pi}}\exp\left[-\frac{(\ln r - \ln r_0)^2}{2s^2}\right] \quad (21)$$

the effective radius and effective variance are given by

$$r_{eff} = r_0 \exp(5s^2/2) \quad (22)$$

$$v_{eff} = \exp(s^2) - 1, \quad (23)$$

TABLE 3. Expansion coefficients a_{nj}, b_{nj}, and c_{nj} for the case of fourth-order ($N = J = 4$) polynomial approximation.

	$n = 0$	1	2	3	4
			a_{nj}		
j					
0	0.94806170E+01	−0.21931424E+02	0.19660563E+01	−0.62014638E−01	0.68698068E−03
1	−0.41634116E+01	0.91221234E+01	−0.80040623E+00	0.24668745E−01	−0.26635909E−03
2	0.68140117E+00	−0.13981211E+01	0.12007009E+00	−0.36040262E−02	0.37704380E−04
3	−0.49433860E−01	0.93819222E−01	−0.78506056E−02	0.22790775E−03	−0.22849189E−05
4	0.13421123E−02	−0.23176709E−02	0.18766039E−03	−0.52080450E−05	0.49035119E−07
			b_{nj}		
j					
0	0.27962992E+03	−0.24032838E+03	0.36339932E+02	−0.16179387E+01	0.21595318E−01
1	−0.11446695E+03	0.10017690E+03	−0.15468189E+02	0.70343154E+00	−0.96306080E−02
2	0.17250787E+02	−0.15317580E+02	0.24187682E+01	−0.11216999E+00	0.15689274E−02
3	−0.11392849E+01	0.10232578E+01	−0.16521647E+00	0.77997602E−02	−0.11109834E−03
4	0.27899660E−01	−0.25266750E−01	0.41692608E−02	−0.20006167E−03	0.28946701E−05
			c_{nj}		
j					
0	0.26993250E+03	−0.21900073E+03	0.34515903E+02	−0.15656232E+01	0.21082708E−01
1	−0.11031200E+03	0.91363848E+02	−0.14724015E+02	0.68250383E+00	−0.94318875E−02
2	0.16589127E+02	−0.13990895E+02	0.23086207E+01	−0.10916428E+00	0.15417866E−02
3	−0.10924881E+01	0.93640279E+00	−0.15818703E+00	0.76165008E−02	−0.10957452E−03
4	0.26655854E−01	−0.23184370E−01	0.40069610E−02	−0.19612247E−03	0.28665195E−05

and the factors $(1 + v_{\text{eff}})(1 + 2v_{\text{eff}})$ and $(1 + v_{\text{eff}})(1 + 2v_{\text{eff}})(1 + 3v_{\text{eff}})$ in expressions (14)–(16) have to be replaced by $(1 + v_{\text{eff}})^2$ and by $(1 + v_{\text{eff}})^3$, respectively (Chýlek et al. 1992). A bimodal size distribution can be treated as a superposition of the lognormal size distributions. The corresponding expressions for the effective radius and the effective variance can be found in Table 1 of Chýlek et al. (1992).

3. Numerical results

The upper part of Fig. 2 shows the absorption coefficient k_{abs} for the case of cumulus and stratus clouds calculated from the exact Mie calculation and integration over the size distribution (solid line) and from the proposed approximation (14). The middle and the lower part of the figure show an error for all cloud types considered to be below 3%. Similarly, the percentage error of the extinction coefficient k_{ext} is below 5% (Fig. 3).

The error in the single-scattering albedo ω_0 is also below 5% except at the wavelength of 12 μm, where the error reaches almost 7% for the case of stratocumulus size distribution (Fig. 4). The slightly larger error of the single-scattering albedo is due to the use of (4) to calculate the albedo from the extinction and absorption coefficients. This implies that the errors in k_{ext} and k_{abs} will add up to give a larger error for the single-scattering albedo.

Finally, Fig. 5 compares the asymmetry factor g obtained from the derived approximation (16) and from the exact Mie calculation. The error is within 1% for all considered cloud types and at all wavelengths within the 8–12-μm interval.

The computer time saved by replacing the Mie calculation, integrated over the size distribution, by the

TABLE 4. Expansion coefficients a_{nj}, b_{nj}, and c_{nj} for the quadratic ($N = J = 2$) approximation.

	$n = 0$	1	2
		a_{nj}	
j			
0	0.23001212E+01	0.45398385E+00	−0.27361086E−01
1	−0.51263886E+00	−0.81865476E−01	0.56357206E−02
2	0.28277523E−01	0.46949275E−02	−0.31701530E−03
		b_{nj}	
j			
0	0.87214441E+01	0.13441900E+01	−0.15449543E+00
1	−0.19858738E+01	−0.61443227E−01	0.21777984E−01
2	0.10672116E+00	−0.30417028E−02	−0.77316651E−03
		c_{nj}	
j			
0	0.57503994E+01	0.66822133E+00	−0.11331277E+00
1	−0.13526513E+01	0.50084508E−01	0.14081642E−01
2	0.72916082E−01	−0.86975960E−02	−0.37865551E−03

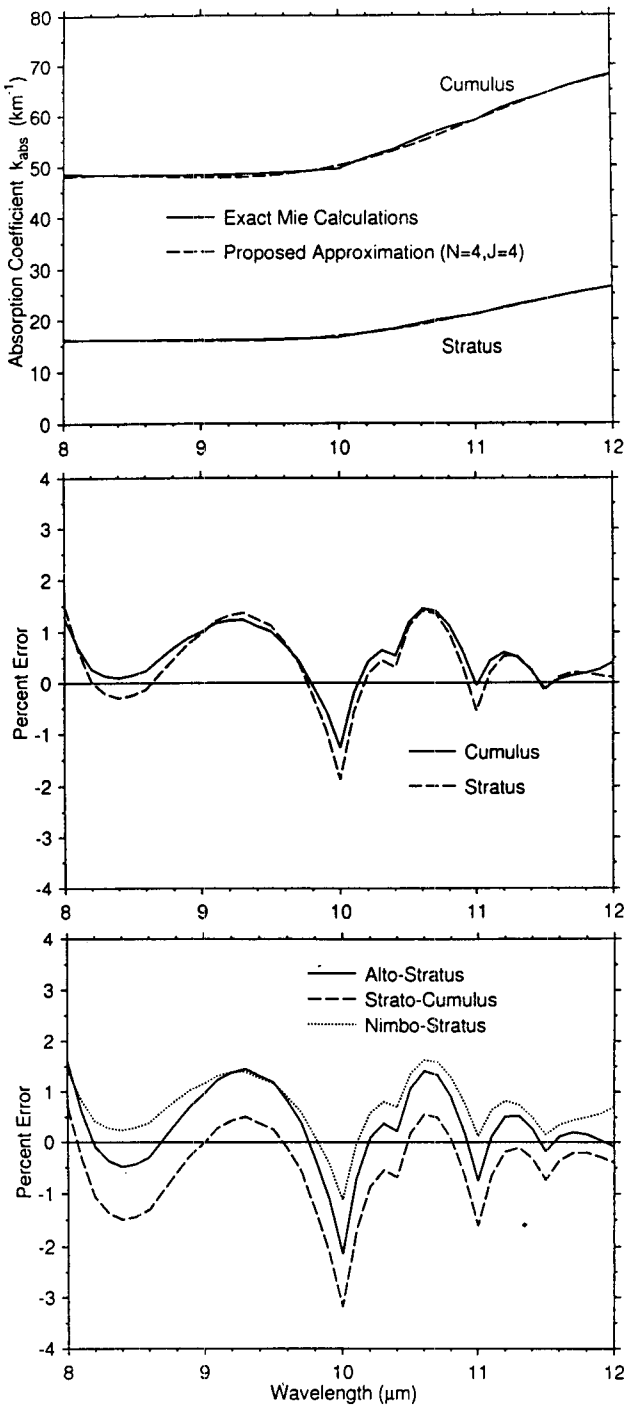

FIG. 2. Comparison of the absorption coefficient k_{abs} calculated using the exact Mie calculation plus integration over the size distribution and the proposed ($N = J = 4$) approximation (14). In the middle and the lower parts of the figure the percentage error for all considered size distributions is shown.

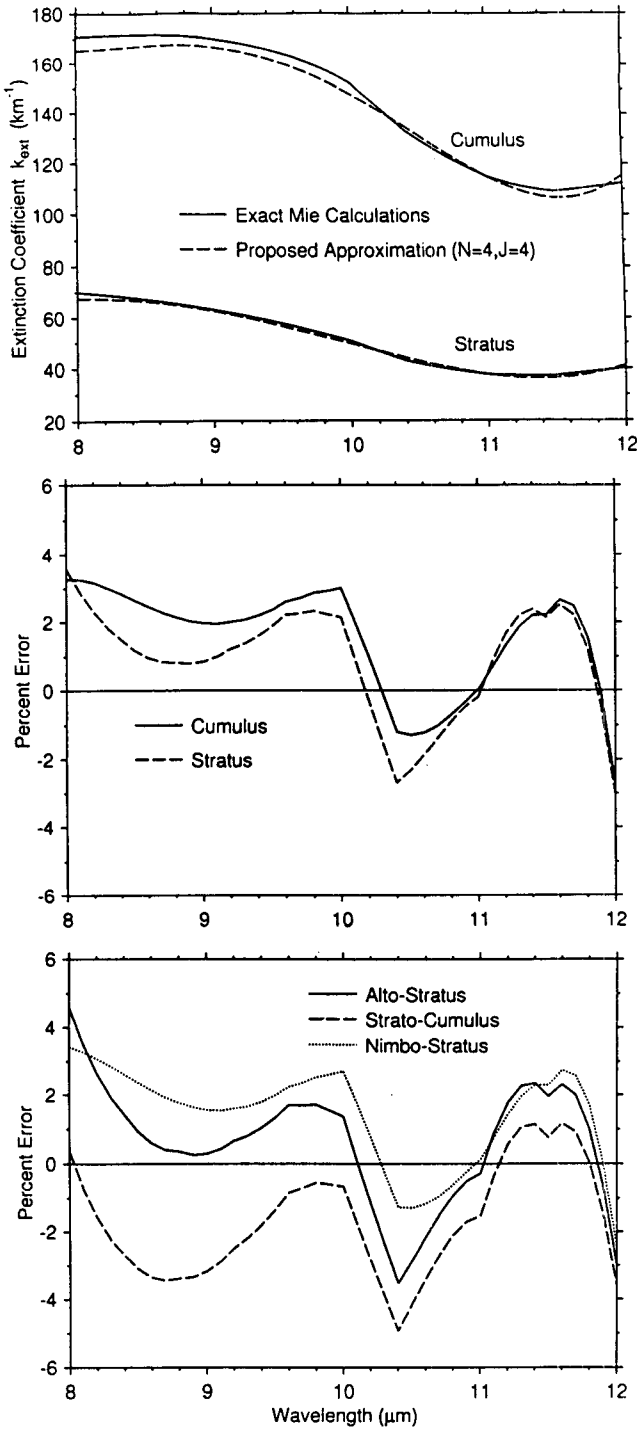

FIG. 3. Comparison and the percentage error of the extinction coefficient k_{ext} in the $N = J = 4$ approximation (15).

developed approximation, is about a factor of 10^2–10^3 depending on the wavelength, the cloud type, and the method of integration.

4. Quadratic approximation

Although relations (14)–(16) for the absorption and extinction coefficients and the asymmetry parameter

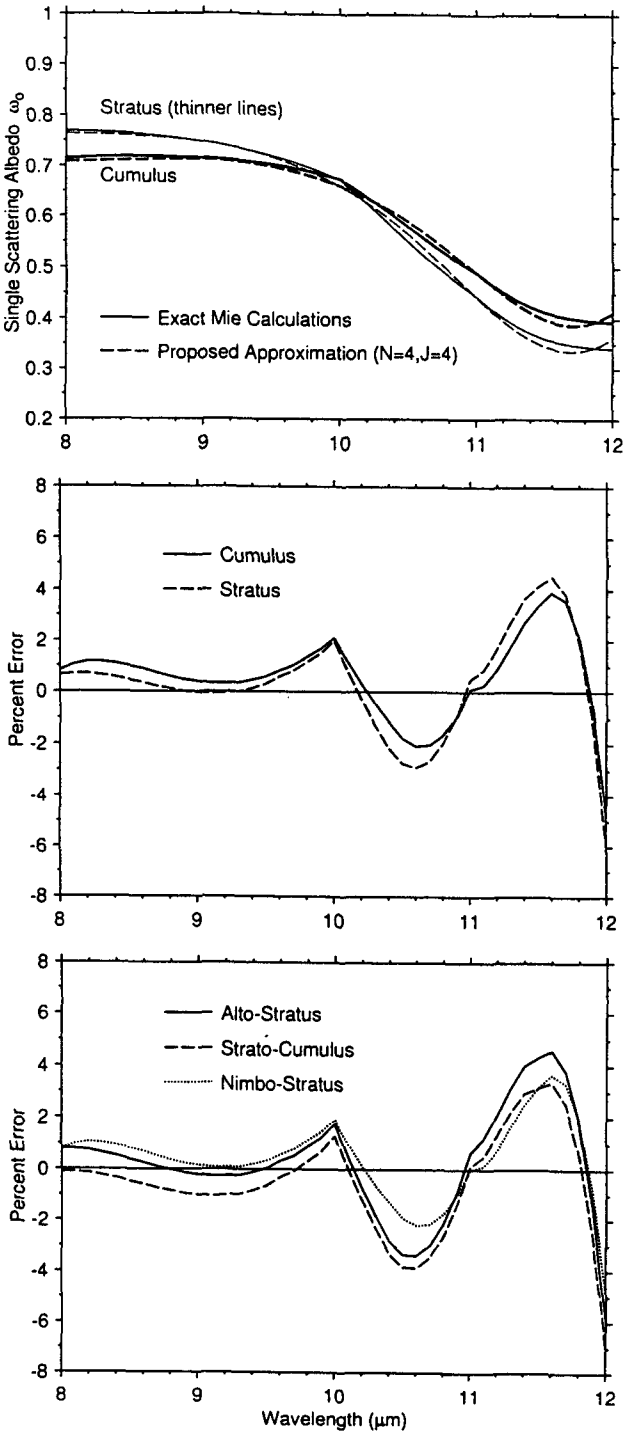

FIG. 4. Comparison and the percentage error of the single-scattering albedo ω_0 in the $N = J = 4$ approximation.

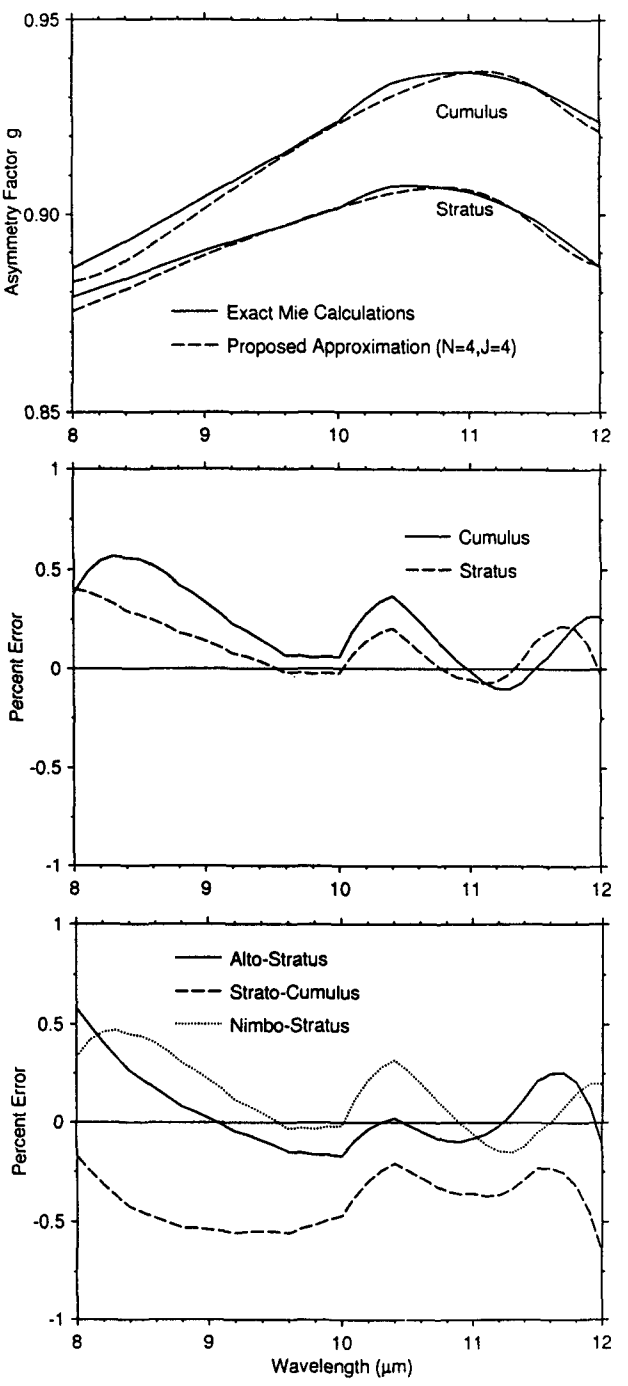

FIG. 5. Comparison and the percentage error of the asymmetry parameter g in the $N = J = 4$ approximation [Eq. (16)].

are computationally fast and simple, they are a bit cumbersome if they are to be carried through in theoretical analysis. For this purpose we may be willing to accept a larger error on the account of simplification of the aforementioned expressions for k_{abs}, k_{ext}, and g.

If the double series expansions (11)–(13) for the Q_{abs}, Q_{ext}, and $(Q_{ext} - Q_{abs})g_r$ are truncated at $N = J = 2$, we obtain

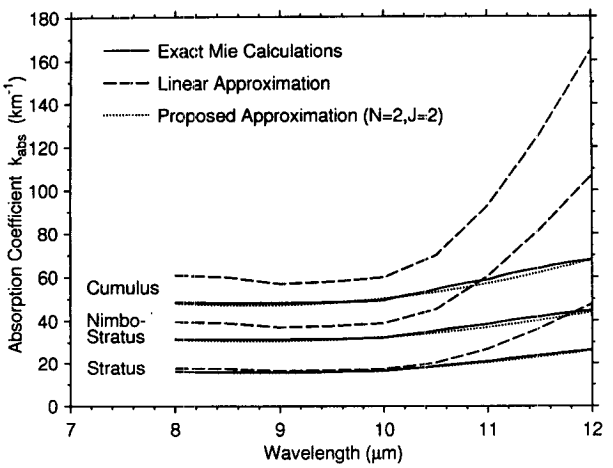

FIG. 6. Comparison of the absorption coefficient k_{abs} obtained using the Mie calculation (solid line), the quadratic (dotted line) approximation [(24) or (27)], and the often-used parameterization as a linear function of liquid water content W (dashed line).

$$k_{abs} = \frac{3W}{4\rho}\left[\frac{1}{r_{eff}}\sum_{j=0}^{2} a_{0j}\lambda^j + \sum_{j=0}^{2} a_{1j}\lambda^j + r_{eff}(1+v_{eff})\sum_{j=0}^{2} a_{2j}\lambda^j\right] \quad (24)$$

$$k_{ext} = \frac{3W}{4\rho}\left[\frac{1}{r_{eff}}\sum_{j=0}^{2} b_{0j}\lambda^j + \sum_{j=0}^{2} b_{1j}\lambda^j + r_{eff}(1+v_{eff})\sum_{j=0}^{2} b_{2j}\lambda^j\right] \quad (25)$$

$$g(k_{ext}-k_{abs}) = \frac{3W}{4\rho}\left[\frac{1}{r_{eff}}\sum_{j=0}^{2} c_{0j}\lambda^j + \sum_{j=0}^{2} c_{1j}\lambda^j + r_{eff}(1+v_{eff})\sum_{j=0}^{2} c_{2j}\lambda^j\right]. \quad (26)$$

The expansion coefficients a_{nj}, b_{nj}, and c_{nj} for $n = 0$, 1, and 2 and $j = 0$, 1, and 2 are given in Table 4. They were obtained from a least-squares fit to the Mie calculation of Q_{abs}, Q_{ext}, and $(Q_{ext} - Q_{abs})g_r$ in the radii range $r < 20$ μm (to obtain a reasonable accuracy with the $N = J = 2$ expansion we had to restrict the droplet sizes to below 20-μm radius).

Using the numerical values of the expansion coefficients (Table 4), (24)–(26) may be rewritten in the form

$$k_{abs} = \frac{3W}{4\rho}\left\{\frac{2.3001}{r_{eff}} + 0.45398 - 0.02736 r_{eff}(1+v_{eff}) - \lambda\left[\frac{0.51264}{r_{eff}} + 0.081865 - 0.0056357 r_{eff}(1+v_{eff})\right] + \lambda^2\left[\frac{0.028278}{r_{eff}} + 0.0046949 - 0.00031702 r_{eff}(1+v_{eff})\right]\right\} \quad (27)$$

with similar expressions for k_{ext} and $g(k_{ext} - k_{abs})$.

Results obtained from the k_{abs} approximation as given by (24) are compared with the exact Mie calculation and integration over the size distribution in Fig. 6. The relative error of k_{abs} for wavelengths between 8 and 12 μm (Table 5) is below 4% for all considered cloud types. The accuracy of 4% is more than sufficient for all practical applications in the field of radiative transfer and climate modeling.

The same or better accuracy is obtained for the cloud infrared emittance (1) as is demonstrated in Table 6. From (1) it follows that

$$\frac{d\epsilon}{\epsilon} = \frac{zk_{abs}}{\exp(zk_{abs}) - 1}\frac{dk_{abs}}{k_{abs}}.$$

Since $zk_{abs} > 0$, we always have $\{zk_{abs}/[\exp(zk_{abs}) - 1]\} < 1$; and we obtain

$$\frac{d\epsilon}{\epsilon} < \frac{dk_{abs}}{k_{abs}}. \quad (28)$$

Thus, the relative error in the emittance ϵ is always smaller than the relative error in the absorption coefficient k_{abs}. This fact is sometimes misunderstood and claims of the relative error in ϵ being larger than that in k_{abs} (because of the exponential dependence) are made. Comparison of infrared emittance (1) calculated using the approximation (24) and the exact Mie calculation is shown in Fig. 7. For comparison, the emit-

TABLE 5. Percentage error $(k_{Mie} - k_{abs})/k_{Mie}$ of the quadratic ($N = J = 2$) k_{abs} approximation [(24) or (27)].

λ (μm)	Stratus	Nimbostratus	Cumulus	Altostratus	Stratocumulus
8.0	−1.6	0.6	0.9	−2.2	−1.8
9.0	2.0	1.0	2.0	2.3	3.2
10.0	−2.7	−2.1	−2.5	−3.0	−3.7
11.0	2.5	3.6	2.3	2.8	3.4
12.0	1.4	1.2	0.1	2.5	4.0

TABLE 6. Percentage error of the emittance ϵ in the quadratic approximation ($N = J = 2$) for the case of stratus, nimbostratus, and cumulus cloud-droplet-size distributions and for the cloud geometrical thickness of 20, 50, and 100 m.

Cloud type:	Stratus			Nimbostratus			Cumulus		
Thickness (m)	20	50	100	20	50	100	20	50	100
Wavelength (μm)									
8	−1.3	−1.0	−0.6	0.4	0.3	0.1	0.5	0.2	0.3
9	1.8	1.4	0.9	1.7	0.4	0.1	0.4	0.2	0.1
10	−2.3	−1.7	−1.0	−1.5	−0.8	−0.5	−1.4	−0.5	−0.1
11	2.0	1.4	0.8	2.0	1.0	0.3	1.2	0.4	0.1
12	1.1	0.7	0.3	0.7	0.3	0.1	0.1	0.1	0.1

tance obtained from (8) (parameterization as a function of W only) is also shown.

The accuracy of the k_{ext} and g in the quadratic approximation [(25) and (26)] is not so good as the accuracy of the absorption coefficient and the emittance. For the considered cloud-droplet-size distributions (Table 1) and the wavelength region of 8–12 μm the errors in the extinction coefficient and the asymmetry factor are within 15% and 12%, respectively.

The error in the single-scattering albedo ω_0 is within 20% in the wavelength interval from 8 to 11.5 μm; however, the error reaches 35% at the wavelength of 12 μm. As mentioned, the larger error in the single-scattering albedo is due to the fact that the albedo is calculated using the developed approximation for extinction and the absorption coefficients. A more accurate approximation for the single-scattering albedo can be developed if the Mie single-particle single-scattering albedo $\omega_0(r)$ is parameterized in a form of a polynomial expansion analogous to expansions (11)–(13).

The usefulness of the quadratic approximation ($N = J = 2$) is mainly in the calculation of the absorption coefficient k_{abs} and the emittance ϵ, both of which are obtained with an error of less than 4%.

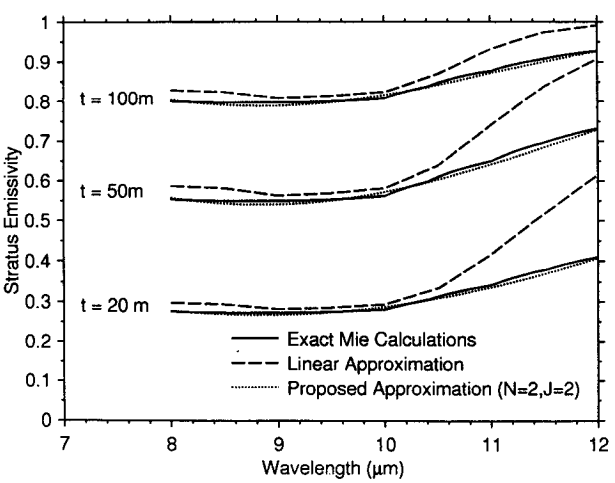

FIG. 7. Stratus emittance for geometrical thickness of the cloud t using the exact Mie calculation (solid line), the quadratic approximation (dotted line), and the often-used linear parameterization of k_{abs} as a linear function of the liquid water content W (dashed line).

5. Summary

We have developed the fourth-order polynomial approximation (in droplet radius and in the wavelength) for the single-droplet absorption efficiency Q_{abs}, extinction efficiency Q_{ext}, and the asymmetry factor in the spectral interval 8–12 μm. These polynomial approximations can be easily integrated over the gamma-type or the lognormal size distributions to provide the scattering characteristics of the cloud of droplets in the form of the absorption coefficient k_{abs}, the extinction coefficient k_{ext}, and the asymmetry parameter g as a function of the wavelength, liquid water content, effective radius, and the effective variance. For the size distributions of typical clouds used in LOWTRAN models the errors in k_{abs}, k_{ext}, and g are less than 3%, 5%, and 1%, respectively. The single-scattering albedo ω_0 can be calculated from the k_{abs} and k_{ext} with the accuracy better than 7%.

The quadratic polynomial approximation for Q_{abs}, Q_{ext}, and g_r leads to errors in k_{abs} of about 4% and in the k_{ext} and g of less than 15%.

Acknowledgments. Reported research was partially supported by the U.S. Army Research Office and by the Atmospheric Environmental Service and the Natural Sciences and Engineering Research Council of Canada. Part of the reported research was done while the first author was visiting the Department of Physics, New Mexico State University.

REFERENCES

Allen, T., 1968: *Particle Size Measurement.* Chapman and Hall, 95–97.

d'Almeida, F. C., P. Koepke, and E. P. Shettle, 1991: *Atmospheric*

Aerosols, Global Climatology and Radiative Characteristics. A. Deepak Publishing, 561 pp.

Chýlek, P., 1978: Extinction and liquid water content of fogs and clouds. *J. Atmos. Sci.*, **35,** 296–300.

——, and V. Ramaswamy, 1982: Simple approximation for infrared emissivity of water clouds. *J. Atmos. Sci.*, **39,** 171–177.

——, P. Damiano, and E. P. Shettle, 1992: Infrared emittance of water clouds. *J. Atmos. Sci.*, **49,** 1459–1472.

Clark, W. E., and K. T. Whitby, 1967: Concentration and size distribution measurements of atmospheric aerosol and text of the theory of self-preserving distributions, *J. Atmos. Sci.*, **24,** 677–687.

Deirmendjian, D., 1969: *Electromagnetic Scattering on Spherical Polydispersions.* Elsevier, 290 pp.

Hansen, J. E., and L. D. Travis, 1974: Light scattering in planetary atmospheres. *Space Sci. Rev.*, **16,** 527–610.

Hunt, G. E., 1973: Radiative properties of terrestrial clouds at visible and infrared thermal window wavelengths. *Quart. J. Roy. Meteor. Soc.*, **99,** 346–369.

Kneizys, F. X., E. P. Shettle, L. W. Abreu, J. H. Chetwynd, G. P. Anderson, W. O. Gallery, J. E. Selby, and S. A. Clough, 1988: Users Guide to LOWTRAN 7, AFGL-TR-88-0177 (available from NTIS AD A206773).

Paltridge, G. W., and C. M. R. Platt, 1976: *Radiative Processes in Meteorology and Climatology.* Elsevier, 318 pp.

Pinnick, R. G., S. G. Jennings, P. Chýlek, and H. J. Auvermann, 1979: Verification of a linear relationship between IR extinction, absorption and liquid water content of fogs. *J. Atmos. Sci.*, **36,** 1577–1586.

Platt, C. M. R., 1976: Infrared absorption and liquid water content in stratocumulus clouds. *Quart. J. Roy. Meteor. Soc.*, **102,** 553–561.

Shettle, E. P., 1989: Models of aerosols, clouds and precipitation for atmospheric propagation studies, pg. 15–1 to 15–13, in AGARD Conference Proceedings CP No. 454, Atmospheric Propagation in the UV, Visible, IR and mm-Wave Region and Related Systems Aspects (available from NTIS N90-21919).

Stephens, G. L., 1984: The parameterization of radiation for numerical weather prediction and climate models. *Mon. Wea. Rev.*, **112,** 826–867.

——, S. C. Tsay, P. W. Stackhouse, and P. J. Flatau, 1990: The relevance of the microphysical and radiative properties of cirrus clouds to climate and climatic feedback. *J. Atmos. Sci.*, **47,** 1742–1753.

van de Hulst, H. C., 1957: *Light Scattering by Small Particles.* Dover, 1981 edition, 470 pp.